Supporting information

Experimental screening and Monte Carlo simulation of Psidium Guajava extract as green inhibitor for carbon steel corrosion in the acidic environment

A.N. El-hoshoudy[1*], E.G. Zaki[1*], S.M. Elsaeed[1] , and K.M. Zohdy[2],

[1]Egyptian Petroleum Research Institute, 11727, Nasr City, Cairo, Egypt.

[2] Higher Technological Institute, 10th of Ramadan City, Cairo, Egypt.

$C_{20}H_{18}O_{11}$

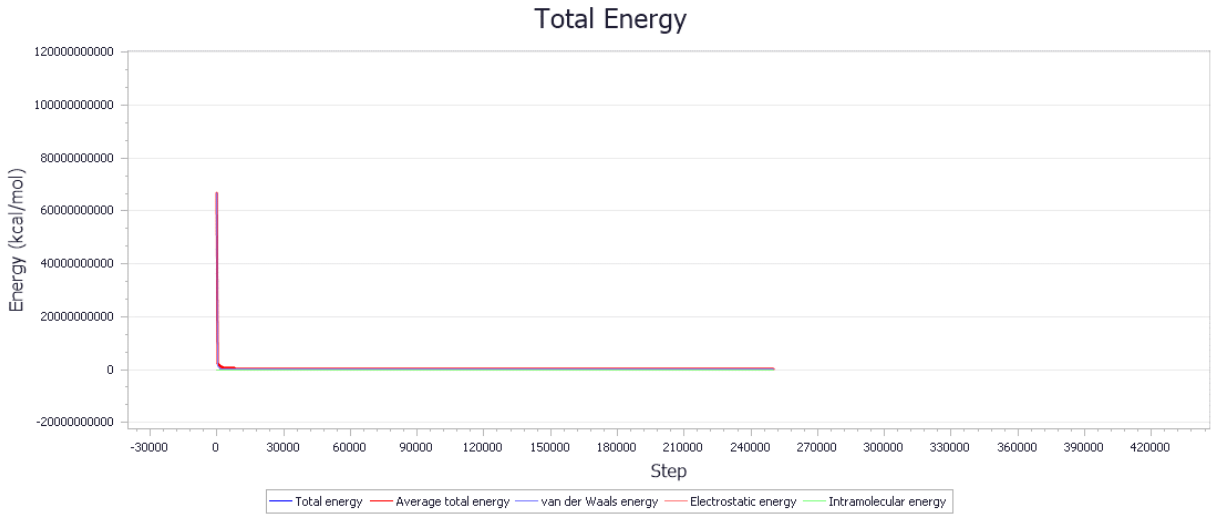

$C_{24}H_{40}O_3$

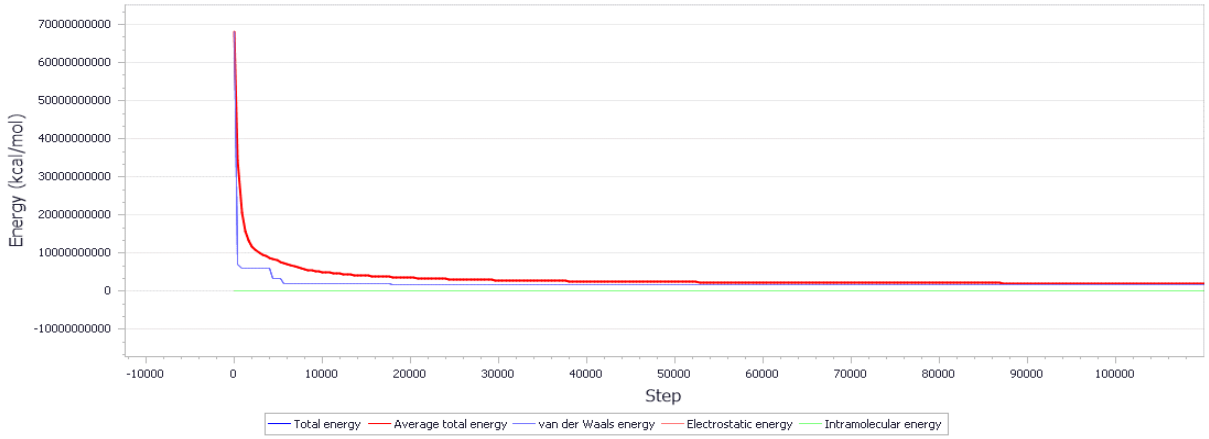

$C_{29}H_{34}O_6$

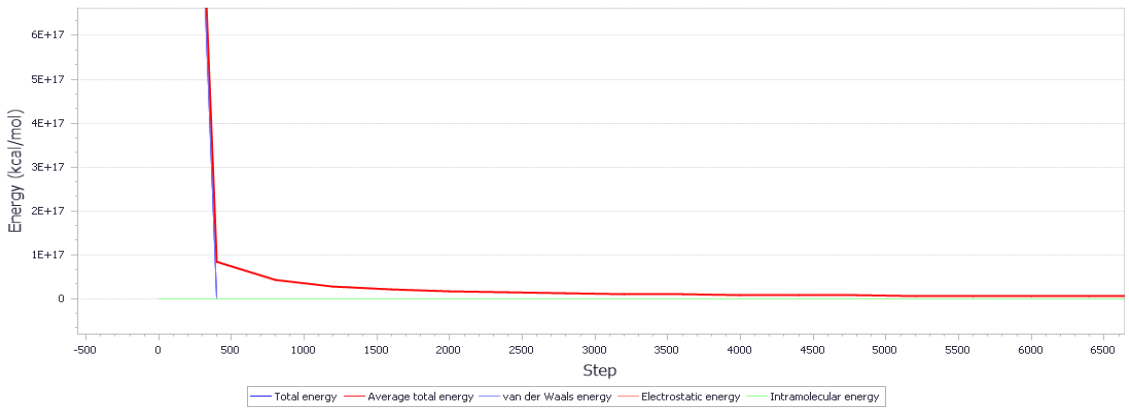

$C_{30}H_{34}O_5$

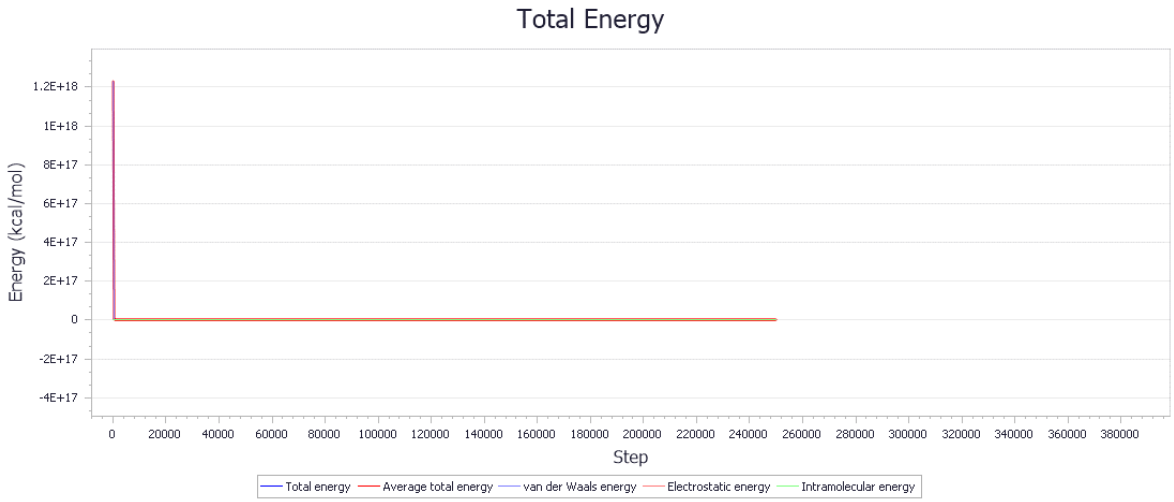

Figure S1: Total energy during adsorption annealing of the four inhibitors on Fe (111) crystal.

$C_{20}H_{18}O_{11}$

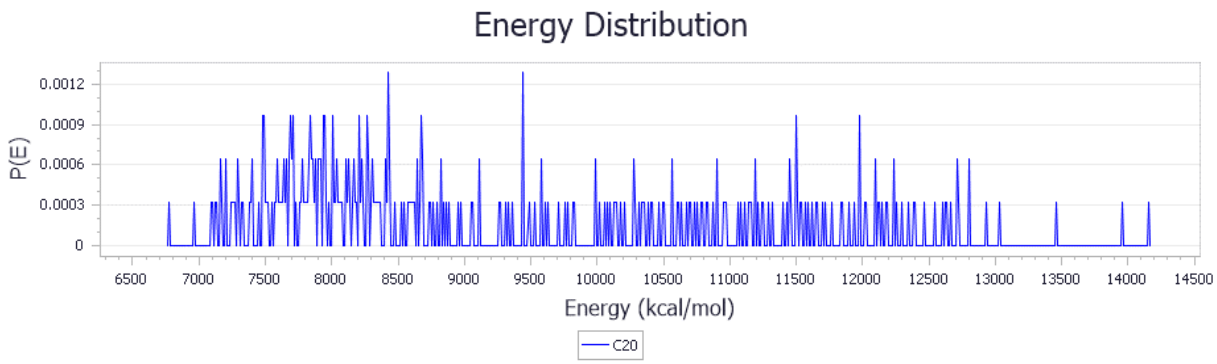

$C_{24}H_{40}O_3$

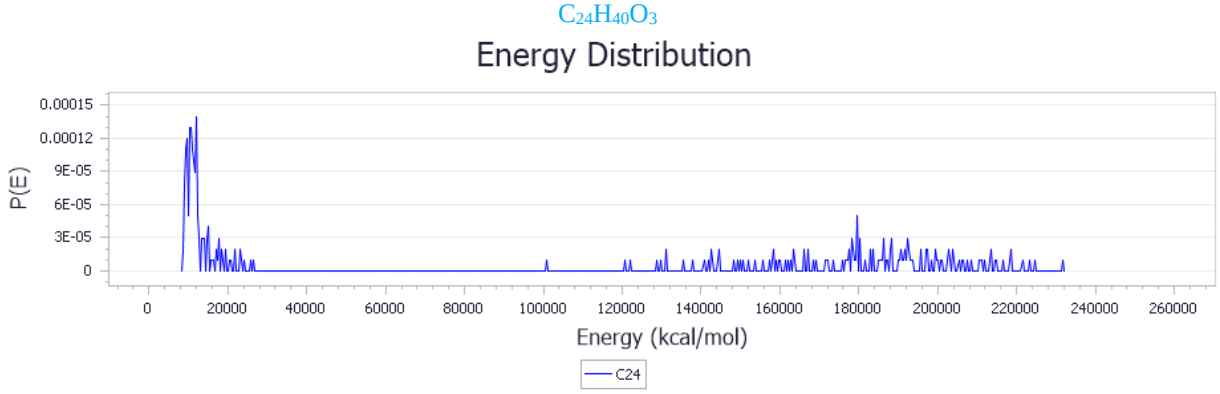

$C_{29}H_{34}O_6$

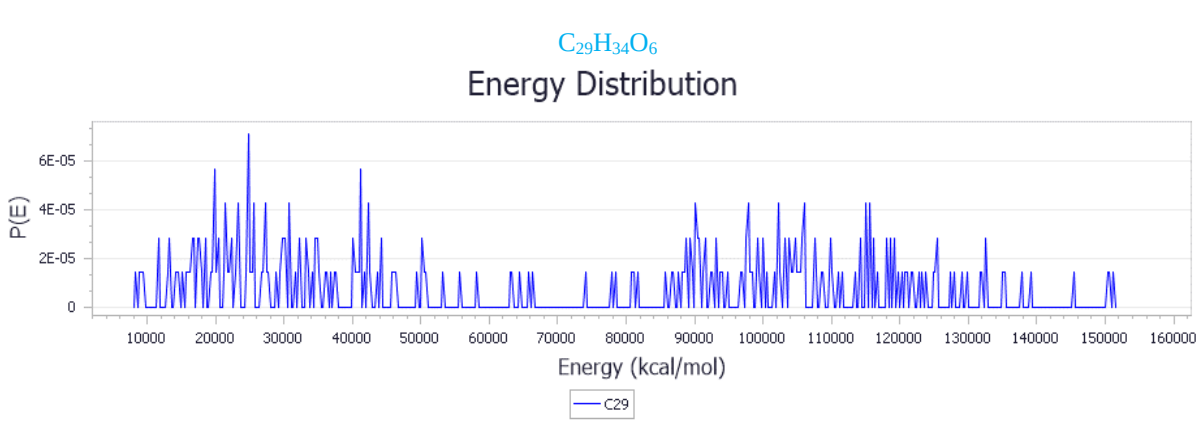

$C_{30}H_{34}O_5$

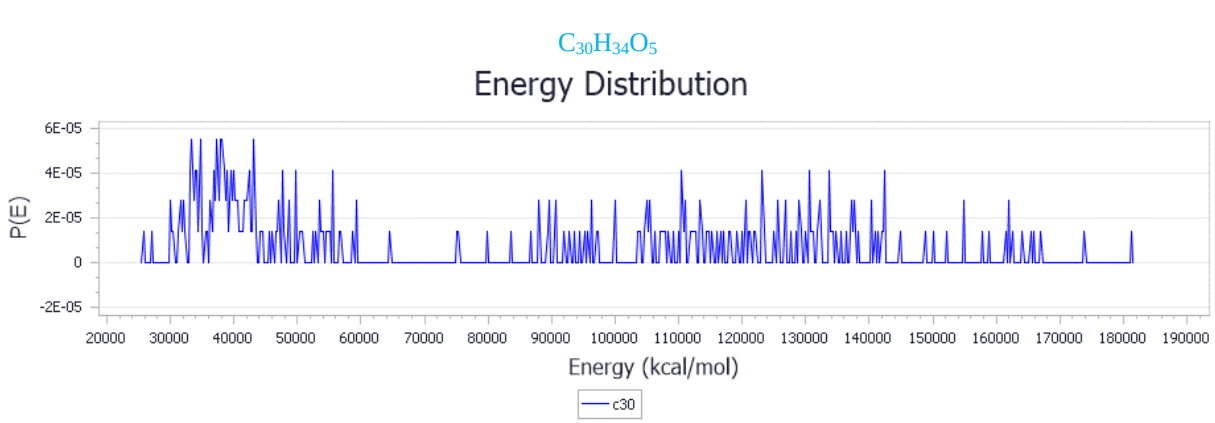

Figure S2: Energy distribution during adsorption annealing of the four inhibitors on Fe (111) crystal.

Table S1: Chemical descriptors computed by the MC simulation for the reported inhibitors

Descriptors by MC simulation for $C_{20}H_{18}O_{11}$

Structures	Total energy, kcal/mol	Adsorption energy kcal/mol	Rigid adsorption energy kcal/mol	Deformation energy kcal/mol	C_{20} : dEad/dNi
Fe (1 1 1) - 1	1.45E+04	1.44E+04	7.15E+03	7.24E+03	7.41E+03
Fe (1 1 1) - 2	1.46E+04	1.45E+04	6.60E+03	7.86E+03	7.77E+03
Fe (1 1 1) - 3	1.49E+04	1.47E+04	6.48E+03	8.25E+03	7.94E+03
Fe (1 1 1) - 4	1.51E+04	1.49E+04	6.64E+03	8.26E+03	8.17E+03
Fe (1 1 1) - 5	1.51E+04	1.50E+04	7.42E+03	7.53E+03	7.78E+03
Fe (1 1 1) - 6	1.52E+04	1.50E+04	6.62E+03	8.42E+03	8.17E+03
Fe (1 1 1) - 7	1.52E+04	1.51E+04	6.80E+03	8.26E+03	7.78E+03
Fe (1 1 1) - 8	1.52E+04	1.51E+04	6.58E+03	8.48E+03	8.04E+03
Fe (1 1 1) - 9	1.52E+04	1.51E+04	7.51E+03	7.57E+03	8.43E+03
Fe (1 1 1) - 10	1.54E+04	1.53E+04	7.25E+03	8.04E+03	7.90E+03
Average	**1.51E+04**	**1.49E+04**	**6.90E+03**	**7.99E+03**	**7.94E+03**

Descriptors by MC simulation for $C_{24}H_{40}O_3$

Structures	**Total energy, kcal/mol**	**Adsorption energy kcal/mol**	**Rigid adsorption energy kcal/mol**	**Deformation energy kcal/mol**	**C_{24} : dEad/dNi**
Fe (1 1 1) - 1	1.17E+05	1.16E+05	4.29E+04	7.33E+04	1.01E+05
Fe (1 1 1) - 2	1.34E+05	1.33E+05	5.00E+04	8.34E+04	1.22E+05
Fe (1 1 1) - 3	1.43E+05	1.42E+05	5.12E+04	9.11E+04	1.31E+05
Fe (1 1 1) - 4	1.44E+05	1.44E+05	5.23E+04	9.17E+04	1.31E+05
Fe (1 1 1) - 5	1.46E+05	1.46E+05	5.12E+04	9.49E+04	1.21E+05
Fe (1 1 1) - 6	1.47E+05	1.47E+05	5.37E+04	9.33E+04	1.36E+05
Fe (1 1 1) - 7	1.48E+05	1.47E+05	5.18E+04	9.54E+04	1.30E+05
Fe (1 1 1) - 8	1.48E+05	1.47E+05	5.42E+04	9.31E+04	1.38E+05
Fe (1 1 1) - 9	1.49E+05	1.49E+05	5.03E+04	9.86E+04	1.29E+05
Fe (1 1 1) - 10	1.51E+05	1.51E+05	5.07E+04	1.00E+05	1.42E+05
Average	**1.43E+05**	**1.42E+05**	**5.08E+04**	**9.15E+04**	**1.28E+05**

Descriptors by MC simulation for $C_{29}H_{34}O_6$

Structures	**Total energy, kcal/mol**	**Adsorption energy kcal/mol**	**Rigid adsorption energy kcal/mol**	**Deformation energy kcal/mol**	**C_{29}: dEad/dNi**
Fe (1 1 1) - 1	1.20E+05	7.51E+04	4.78E+04	2.73E+04	6.32E+04
Fe (1 1 1) - 2	1.32E+05	8.77E+04	5.52E+04	3.24E+04	8.11E+04
Fe (1 1 1) - 3	1.36E+05	9.09E+04	5.83E+04	3.27E+04	7.39E+04
Fe (1 1 1) - 4	1.38E+05	9.32E+04	5.70E+04	3.62E+04	7.79E+04
Fe (1 1 1) - 5	1.43E+05	9.80E+04	5.85E+04	3.95E+04	8.10E+04
Fe (1 1 1) - 6	1.47E+05	1.02E+05	6.29E+04	3.90E+04	8.84E+04
Fe (1 1 1) - 7	1.47E+05	1.02E+05	5.56E+04	4.66E+04	9.24E+04
Fe (1 1 1) - 8	1.48E+05	1.03E+05	5.92E+04	4.35E+04	9.01E+04

Fe (1 1 1) - 9	1.50E+05	1.05E+05	6.02E+04	4.51E+04	9.92E+04
Fe (1 1 1) - 10	1.51E+05	1.06E+05	5.84E+04	4.77E+04	8.17E+04
Average	**1.41E+05**	**9.63E+04**	**5.73E+04**	**3.90E+04**	**8.29E+04**
Descriptors by MC simulation for $C_{30}H_{34}O_5$					
Structures	**Total energy, kcal/mol**	**Adsorption energy kcal/mol**	**Rigid adsorption energy kcal/mol**	**Deformation energy kcal/mol**	**C_{30} : dEad/dNi**
Fe (1 1 1) - 1	1.10E+05	1.07E+05	4.35E+04	6.33E+04	7.53E+04
Fe (1 1 1) - 2	1.13E+05	1.10E+05	4.71E+04	6.25E+04	7.52E+04
Fe (1 1 1) - 3	1.16E+05	1.12E+05	4.54E+04	6.70E+04	8.00E+04
Fe (1 1 1) - 4	1.20E+05	1.16E+05	4.52E+04	7.11E+04	8.80E+04
Fe (1 1 1) - 5	1.21E+05	1.18E+05	5.44E+04	6.31E+04	8.95E+04
Fe (1 1 1) - 6	1.25E+05	1.22E+05	4.97E+04	7.20E+04	8.68E+04
Fe (1 1 1) - 7	1.26E+05	1.23E+05	5.15E+04	7.13E+04	8.37E+04
Fe (1 1 1) - 8	1.26E+05	1.23E+05	4.95E+04	7.33E+04	8.81E+04
Fe (1 1 1) - 9	1.26E+05	1.23E+05	4.69E+04	7.59E+04	8.94E+04
Fe (1 1 1) - 10	1.27E+05	1.23E+05	5.03E+04	7.27E+04	9.03E+04
Average	**1.21E+05**	**1.18E+05**	**4.84E+04**	**6.92E+04**	**8.46E+04**

Table S2: Summary of MC simulation in case of $C_{20}H_{18}O_{11}$

```
Module                    : Adsorption Locator
Version                   : 2017
Build date                : May  5 2016
Host                      : DESKTOP-T7700NS
Operating system          : Windows
Task started              : Fri Aug 23 19:55:00 2019
Random number seed        : 1406689333
---- Simulated annealing calculation parameters ----
Loading steps             : 100000
Heating cycles            : 5
Steps per cycle           : 50000
Optimize geometry         : yes
---- Energy parameters ----
Forcefield                : Universal
Charges                   : Use current
Electrostatic terms:
  Summation method        : Ewald & Group
  Accuracy                : 0.0001 kcal/mol
  Charge group cutoff     : 15.5 A
  Buffer width            : 0.5 A
van der Waals terms:
  Summation method        : Atom based
  Truncation method       : Cubic spline
  Cutoff distance         : 15.5 A
  Spline width            : 1 A
  Buffer width            : 0.5 A
---- Simulated annealing ----
Automatic                 : yes
Adjust Monte Carlo step sizes   : yes
---- Simulated annealing calculation ----
Framework charge          : 0.000 e per cell
Loading steps used        : 13
---- Monte Carlo steps ----
| Sorbate     | Regrowth    | Rotation    | Translation |
|             | steps       | steps       | steps       |
|_____________|_____________|_____________|_____________|
| C20         |             |             |             |
|  Accepted   |           1 |        4143 |       25806 |
|  Attempted  |       11765 |      119053 |      119182 |
|  Ratio      |  8.500e-005 |       0.035 |       0.217 |
---- Isosteric heats ----
| Sorbate     | Average     | Minimum     | Maximum     |
|             | kcal/mol    | kcal/mol    | kcal/mol    |
|_____________|_____________|_____________|_____________|
| C20         |   -9301.156 |  -14109.059 |   -6729.059 |
---- Overall system energies ----
Average total energy      : -214748.365 kcal/mol
---- Step sizes ----
| Sorbate     | Rotate      | Translate |
|             | degrees     | Angstrom  |
|_____________|_____________|___________|
| C20         |       0.500 |     0.500 |
Task terminated           : Fri Aug 23 21:14:19 2019
Total CPU time used       : 1:18:49 hours
Termination status        : Normal
```

Table S3: Summary of MC simulation in case of $C_{24}H_{40}O_3$

```
Module                    : Adsorption Locator
Version                   : 2017
Build date                : May  5 2016
Host                      : DESKTOP-T7700NS
Operating system          : Windows
Task started              : Sat Aug 31 16:04:19 2019
Random number seed        : 195807721
---- Simulated annealing calculation parameters ----
Loading steps             : 100000
Heating cycles            : 5
Steps per cycle           : 50000
Optimize geometry         : yes
---- Energy parameters ----
Forcefield                : Universal
Charges                   : Use current
Electrostatic terms:
  Summation method        : Ewald & Group
  Accuracy                : 0.0001 kcal/mol
  Charge group cutoff     : 15.5 A
  Buffer width            : 0.5 A
van der Waals terms:
  Summation method        : Atom based
  Truncation method       : Cubic spline
  Cutoff distance         : 15.5 A
  Spline width            : 1 A
  Buffer width            : 0.5 A
---- Simulated annealing ----
Automatic                 : yes
Adjust Monte Carlo step sizes   : yes
---- Simulated annealing calculation ----
Framework charge          : 0.000 e per cell
Loading steps used        : 15
---- Monte Carlo steps ----
| Sorbate    | Regrowth   | Rotation   | Translation |
|            | steps      | steps      | steps       |
|____________|____________|____________|_____________|
| C24        |            |            |             |
|  Accepted  |          0 |       2037 |       26056 |
|  Attempted |      11928 |     119009 |      119063 |
|  Ratio     |      0.000 |      0.017 |       0.219 |
---- Isosteric heats ----
| Sorbate    | Average    | Minimum    | Maximum    |
|            | kcal/mol   | kcal/mol   | kcal/mol   |
|____________|____________|____________|____________|
| C24        | -96815.843 | -231928.306 |  -8931.906 |
---- Overall system energies ----
Average total energy      : -214748.365 kcal/mol
---- Step sizes ----
| Sorbate    | Rotate     | Translate |
|            | degrees    | Angstrom  |
|____________|____________|___________|
| C24        |      0.500 |     0.500 |
Task terminated           : Sat Aug 31 20:55:27 2019
Total CPU time used       : 4:44:15 hours
Termination status        : Normal
```

Table S4: Summary of MC simulation in case of $C_{29}H_{34}O_6$

```
Module                        : Adsorption Locator
Version                       : 2017
Build date                    : May  5 2016
Host                          : DESKTOP-T7700NS
Operating system              : Windows
Task started                  : Sat Aug 24 04:14:15 2019
Random number seed            : 174734347
---- Simulated annealing calculation parameters ----
Loading steps                 : 100000
Heating cycles                : 5
Steps per cycle               : 50000
Optimize geometry             : yes
---- Energy parameters ----
Forcefield                    : Universal
Charges                       : Use current
Electrostatic terms:
  Summation method            : Ewald & Group
  Accuracy                    : 0.0001 kcal/mol
  Charge group cutoff         : 15.5 A
  Buffer width                : 0.5 A
van der Waals terms:
  Summation method            : Atom based
  Truncation method           : Cubic spline
  Cutoff distance             : 15.5 A
  Spline width                : 1 A
  Buffer width                : 0.5 A
---- Simulated annealing ----
Automatic                     : yes
Adjust Monte Carlo step sizes   : yes
---- Simulated annealing calculation ----
Framework charge              : 0.000 e per cell
Loading steps used            : 2148
---- Monte Carlo steps ----
| Sorbate     | Regrowth    | Rotation    | Translation |
|             | steps       | steps       | steps       |
|_____________|_____________|_____________|_____________|
| C29         |             |             |             |
|  Accepted   |           0 |         316 |       24986 |
|  Attempted  |       12042 |      119232 |      118726 |
|  Ratio      |       0.000 |  2.650e-003 |       0.210 |
---- Isosteric heats ----
| Sorbate     | Average     | Minimum     | Maximum     |
|             | kcal/mol    | kcal/mol    | kcal/mol    |
|_____________|_____________|_____________|_____________|
| C29         |  -68472.020 | -151274.197 |   -8454.997 |
---- Overall system energies ----
Average total energy          : -214748.365 kcal/mol
---- Step sizes ----
| Sorbate     | Rotate      | Translate |
|             | degrees     | Angstrom  |
|_____________|_____________|___________|
| C29         |       0.500 |     0.500 |
Task terminated               : Sat Aug 24 06:10:16 2019
Total CPU time used           : 1:55:23 hours
Termination status            : Normal
```

Table S5: Summary of MC simulation in case of $C_{30}H_{34}O_5$

```
Module                    : Adsorption Locator
Version                   : 2017
Build date                : May  5 2016
Host                      : DESKTOP-T7700NS
Operating system          : Windows
Task started              : Fri Aug 23 21:36:10 2019
Random number seed        : 15501347
---- Simulated annealing calculation parameters ----
Loading steps             : 100000
Heating cycles            : 5
Steps per cycle           : 50000
Optimize geometry         : yes
---- Energy parameters ----
Forcefield                : Universal
Charges                   : Use current
Electrostatic terms:
  Summation method        : Ewald & Group
  Accuracy                : 0.0001 kcal/mol
  Charge group cutoff     : 15.5 A
  Buffer width            : 0.5 A
van der Waals terms:
  Summation method        : Atom based
  Truncation method       : Cubic spline
  Cutoff distance         : 15.5 A
  Spline width            : 1 A
  Buffer width            : 0.5 A
---- Simulated annealing ----
Automatic                 : yes
Adjust Monte Carlo step sizes   : yes
---- Simulated annealing calculation ----
Framework charge          : 0.000 e per cell
Loading steps used        : 167
---- Monte Carlo steps ----
| Sorbate    | Regrowth   | Rotation   | Translation |
|            | steps      | steps      | steps       |
|_____________________________________________________
| c30        |            |            |             |
|  Accepted  |          0 |        232 |       28533 |
|  Attempted |      12088 |     118651 |      119261 |
|  Ratio     |      0.000 |  1.955e-003 |       0.239 |
---- Isosteric heats ----
| Sorbate    | Average    | Minimum    | Maximum    |
|            | kcal/mol   | kcal/mol   | kcal/mol   |
|_____________________________________________________
| c30        |  -81727.121 | -181363.033 |  -25867.033 |
---- Overall system energies ----
Average total energy      : -214748.365 kcal/mol
---- Step sizes ----
| Sorbate    | Rotate   | Translate |
|            | degrees  | Angstrom  |
|_____________________________________
| c30        |    0.500 |     0.500 |
Task terminated           : Fri Aug 23 23:32:36 2019
Total CPU time used       : 1:55:56 hours
Termination status        : Normal
```

Frontier molecular orbitals (FMO) energies (E_{HOMO} & E_{LUMO}): energies of the highest occupied molecular orbitals, and the lowest unoccupied molecular orbitals respectively, and used to forecast the adsorption centers (interaction sites) of the inhibitors. E_{HOMO} (electron-donor) is associated with the electron-donating ability of the inhibitors molecules [1] to the unoccupied (d-orbital) of the metal surface, while E_{LUMO} (electron-acceptor), is the lowest energetic orbital which receives electrons [2]. Based on Koopman's theorem [3], the E_{HOMO} & E_{LUMO} were formulated to the ionization potential and the electron affinity respectively[4, 5].

Ionization potential (I): It is expressed as the required energy for electron removal from the neutral atom and describes the molecule chemical reactivity. Higher ionization energies reveal higher stability and chemical inertness, and vice versa [6].

$$I \approx -E_{HOMO} \quad (5)$$

Electron affinity (A): It is the released energy during the electron acceptance by a neutral atom to form an anion. The ionization potential and the electron affinity were correlated to the electronegativity values

$$A \approx -E_{LUMO} \quad (6)$$

The energy bandgap ($\Delta E_{LUMO\text{-}HOMO}$): is the energy discrepancy between E_{LUMO} and E_{HOMO} orbitals and it is a remarkable stability index towards the inhibitor molecule reactivity on the metal surface [7]. Lower values of energy gap imply that the molecule is soft, polarizable, and exhibits better corrosion performance [1] since the electron removing energy from the E_{HOMO} orbitals will be lower value. Polarizable atoms easily give electrons to the metal surface while unpolarizable one is hardly given electron to metal.

$$\Delta E_{gap} = E_{LUMO} - E_{HOMO} \quad (7)$$

Absolute electronegativity (χ): higher electronegativities designate lower electron-donating tendency of the inhibitor to the metallic surface which in turn weakened the coordinate bonds between the inhibitor and the reactive spots on the metallic surface, so, reduce the adsorption and inhibition performance [8].

$$\chi = -\frac{1}{2}(E_{LUMO} + E_{HOMO}) = (\frac{I + A}{2}) \quad (8)$$

Global hardness (η): Global hardness and softness are significant descriptors to quantify the stability, firmness, and reactivity of the molecule's inhibition efficiencies. The soft concept signifies polarizable chemical moieties and a hard concept denotes unpolarizable chemical one. Chemical hardness specifies that the inhibitor molecule hardly deforms the electronic cloud [9]. Since chemical hardness is related to the energy bandgap ($\Delta E_{LUMO\text{-}HOMO}$) *according to* Koopman's theorem. Consequently, By hardness increase, the

adsorbed molecules have a higher energy gap, and in turn, have little capability to adapt suitably to the metallic surface, so cover small surface area [10].

$$\eta = \frac{I - A}{2} \quad (9)$$

Global softness (σ): for ease electrons transfer, the adsorption process occurs at the reactive positive sites on the metal, where the softness has the highest value (i.e. higher softness implies the molecule has high polarizability and can easily adsorb on the metallic surface) [11]. The softness augmented by increasing the number of hydrophobic moieties, owing to the increasing molecule electron-donation, so it increases the transferred electron amounts from the donor molecule (inhibitors) to the acceptors (metallic surface) so adsorption propensity increases on the metal surface [8, 12]. Based on $\Delta E_{LUMO-HOMO}$ calculations, soft molecules have a small $\Delta E_{LUMO-HOMO}$, where the softness and hardness are related diversely to each other [8].

$$\sigma = \frac{1}{\eta} \quad (10)$$

Global electrophilicity index (ω): electrophilicity measures the reactivity of electrons attraction from a nucleophilic chemical species. Maynard and co-workers proposed an electrophilicity index which estimates the tendency of inhibitors to acquire electrons [13]. The greater value of (ω) reveals the greater molecule capacity to receive electrons and thus acts as an electrophile and vice versa [5].

$$\omega = \frac{\mu^2}{2\eta} \quad (11)$$

Nucleophilicity (ε): is a physical inverse of electrophilicity [14]. Molecules with higher electrophilicity are ineffective corrosion inhibitors while molecules with large nucleophilicity act as effective corrosion inhibitors [14].

$$\varepsilon = \frac{1}{\omega} \quad (12)$$

Electronic chemical potential (μ):

$$\mu = -\chi \quad (13)$$

The dipole moment (Ψ): The dipole moment describes the electronic distribution and molecule polarity. As the dipole moment increases, the polar characteristics of the molecule increase. High values of dipole moment indicate ease molecule adsorption and good inhibition proficiency by adjusting the electron transfer in the adsorbed layer [15].

The fraction of electron transferred (ΔN) from the inhibitor molecules to the iron surface was computed corresponding to the Pearson electronegativity scale [16, 17] as the electrons will flow from the inhibitor surface to metallic iron (Fe) surface until equilibrated chemical potentials reached [5, 18]. It is observed that electron transfer increases by increasing the inhibitor electronegativity [14].

$$\Delta N = \frac{\chi_{Fe} - \chi_{inh}}{2(\eta_{Fe} + \eta_{inh})} \qquad (14)$$

Where, χ_{Fe} & χ_{inh} are the absolute electronegativities of the iron and inhibitor molecules respectively, while η_{Fe} & η_{inh} are the absolute hardness of iron and inhibitor molecule respectively [13, 14]. In the current study, the typical theoretical values χ_{Fe} = 7.0 eV/mol, and η_{Fe}=0.0 eV/mol [5, 9] were implemented.

***ΔE Back-donation* (Total energy change, Δ*TE*)**; This descriptor describes two reversible processes. Firstly, the electron donation from the inhibitor molecule to the vacant *d-orbitals* in the (Fe) through the electron-donating process. secondly, electron receiving from occupied d-orbitals in the (Fe) metal surface to the active sites on the inhibitor molecules through the electron-back-donation [5]. It is calculated as a function of chemical hardness;

$$\Delta E_{Back-donation} = -\frac{\eta}{4} \qquad (15)$$

1. K. Zakaria, N. Negm, E. Khamis and E. Badr, *Journal of The Taiwan Institute of Chemical Engineers*, 2016, **61**, 316-326.
2. D. Özkır, K. Kayakırılmaz, E. Bayol, A. A. Gürten and F. Kandemirli, *Corros. Sci.*, 2012, **56**, 143-152.
3. Y. ELouadi, F. Abrigach, A. Bouyanzer, R. Touzani, O. Riant, B. ElMahi, A. El Assyry, S. Radi, A. Zarrouk and B. Hammouti, *Der Pharma Chemica*, 2015, **7**, 265-275.
4. G. Gece and S. Bilgiç, *Corros. Sci.*, 2010, **52**, 3304-3308.
5. I. Obot, I. B. Onyeachu, N. Wazzan and A. H. Al-Amri, *J. Mol. Liq.*, 2019, **279**, 190-207.
6. A. Rosen and B. Wästberg, *J. Am. Chem. Soc.*, 1988, **110**, 8701-8703.
7. H. Ju, Z.-P. Kai and Y. Li, *Corros. Sci.*, 2008, **50**, 865-871.
8. N. Negm, M. Migahed, R. Farag, A. Fadda, M. Awad and M. Shaban, *J. Mol. Liq.*, 2018, **262**, 363-375.

9. M. Bedair, S. Soliman, M. Hegazy, I. Obot and A. Ahmed, *J. Adhes. Sci. Technol.*, 2019, **33**, 1139-1168.
10. D. Tabor, *Review of physics in technology*, 1970, **1**, 145.
11. I. Lukovits, E. Kalman and F. Zucchi, *Corrosion*, 2001, **57**, 3-8.
12. G. Gao and C. Liang, *Electrochim. Acta*, 2007, **52**, 4554-4559.
13. E. A. Gad, E. Azzam and S. A. Halim, *Egyptian journal of petroleum*, 2017.
14. S. Kaya, B. Tüzün, C. Kaya and I. B. Obot, *Journal of the Taiwan Institute of Chemical Engineers*, 2016, **58**, 528-535.
15. M. Behpour, S. Ghoreishi, N. Soltani, M. Salavati-Niasari, M. Hamadanian and A. Gandomi, *Corros. Sci.*, 2008, **50**, 2172-2181.
16. R. G. Pearson, *Inorg. Chem.*, 1988, **27**, 734-740.
17. I. Obot and N. Obi-Egbedi, *Corros. Sci.*, 2010, **52**, 657-660.
18. A. Y. Musa, R. T. Jalgham and A. B. Mohamad, *Corros. Sci.*, 2012, **56**, 176-183.